Review

Review of Adsorption Studies for Contaminant Removal from Wastewater Using Molecular Simulation

Noor e Hira [1], Serene Sow Mun Lock [1,*], Noor Fazliani Shoparwe [2], Irene Sow Mei Lock [3], Lam Ghai Lim [4], Chung Loong Yiin [5,6], Yi Herng Chan [7] and Muhammad Hassam [8]

[1] CO2 Research Center (CO2RES), Department of Chemical Engineering, Universiti Teknologi PETRONAS, Seri Iskandar 32610, Malaysia

[2] Gold Rare Earth and Material Technopreneurship Centre, Faculty of Bioengineering and Technology, Jeli Campus, Universiti Malaysia Kelantan, Jeli 17600, Malaysia

[3] Group Technical Solutions, Project Delivery and Technology Division, PETRONAS, Kuala Lumpur 50088, Malaysia

[4] School of Engineering, Monash University Malaysia, Bandar Sunway 47500, Malaysia

[5] Department of Chemical Engineering and Energy Sustainability, Faculty of Engineering, Universiti Malaysia Sarawak (UNIMAS), Kota Samarahan 94300, Malaysia

[6] Institute of Renewable and Sustainable Energy (ISuRE), Universiti Malaysia Sarawak (UNIMAS), Kota Samarahan 94300, Malaysia

[7] PETRONAS Research Sdn. Bhd. (PRSB), Lot 3288 & 3289, Off Jalan Ayer Itam, Kawasan Institusi Bangi, Kajang 43000, Malaysia

[8] Department of Food Science and Technology, University of Central Punjab, Lahore 54782, Pakistan

* Correspondence: sowmun.lock@utp.edu.my

Abstract: In recent years, simulation studies have emerged as valuable tools for understanding processes. In particular, molecular dynamic simulations hold great significance when it comes to the adsorption process. However, comprehensive studies on molecular simulations of adsorption processes using different adsorbents are scarcely available for wastewater treatment covering different contaminants and pollutants. Hence, in this review, we organized the available information on various aspects of the adsorption phenomenon that were realized using molecular simulations for a broad range of potentially effective adsorbents applied in the removal of contaminants from wastewater. This review was compiled for adsorbents under five major categories: (1) carbon-based, (2) oxides and hydroxides, (3) zeolites, (4) metal–organic frameworks and (5) clay. From the review, it was found that simulation studies help us understand various parameters such as binding energy, Gibbs free energy, electrostatic field, ultrasound waves and binding ability for adsorption. Moreover, from the review of recent simulation studies, the effect of ultrasound waves and the electrostatic field was elucidated, which promoted the adsorption capacity. This review can assist in the screening of classified adsorbents for wastewater treatment using a fast and cheap approach while helping us understand the adsorption process from an atomistic perspective.

Keywords: adsorption; wastewater treatment; molecular simulation; adsorption capacity; carbon-based compounds; oxides and hydroxides; zeolites; metal–organic frame; clay

1. Introduction

Adsorption is the most promising technique to remove contaminants from wastewater. There are many different technologies used to remove contaminants or pollutants from wastewater, but adsorption is regarded as the most suitable and effective technique due to its high efficiency and low cost [1,2]. Various types of adsorbents have been introduced for the adsorption process, including zeolites, oxides and hydroxides, carbon-based, metal–organic frameworks and clay. Each adsorbent has potential benefits and tends to remove specific contaminants from wastewater. Adsorption is a surface phenomenon, and these adsorbents sorb the contaminants on their surface to remove them from wastewater.

Industrial wastewater incorporating different contaminants is treated using these adsorbents since they may contain dyes, pharmaceutical residues, pesticides and organic and inorganic pollutants [3–5]. These pollutants are toxic and can cause serious damage to human health. If industrial wastewater smears the natural water, it can cause consequential harm to all living organisms [6]. Every industry is responsible for the correct disposal of wastewater after its treatment. According to the Environmental Protection Agency (EPA), all water pollutants are unacceptable in wastewater over a certain amount and must be removed to protect the environment and to comply with regulations [7]. In this era, wastewater treatment has become a separate field where effective and valuable treatment methods are introduced and applied after it [8]. The adsorption method has been employed for wastewater purification and specifically for industrial effluent treatment since decades ago. Almost 20 years back, G.M. Walker [9] studied dye adsorption on activated carbon and reported an adsorption capacity of 537, 535 and 852 mg/g for dyes TB4R (Tectilon Blue 4R-01), TR2B (Tectilon Red 2B) and TO3G (Tectilon Orange 3G), respectively. Paliulis [10] studied the adsorption of harmful organic pollutants present in industrial wastewater using zeolite. Natural zeolite, which was constituted by clinoptilolite and mordenite minerals, was selected for studying the adsorption of formaldehyde, and the adsorption efficiency was obtained in the range of 19% to 85% [10]. A vast myriad of experiments has been performed to study adsorption in wastewater treatment [11], which provided promising results to expand its use in the industry. McKay studied low-cost adsorbents for dye removal from wastewater as large textile industries were concerned about utilizing affordable materials [12]. McKay proved that bentonite clay was the best adsorbent with a cation–anion exchange capacity of 1.25 and 2.3 per 100 mg [12]. However, the commercial application of these adsorbents is still limited so far majorly due to a limited understanding of the adsorption mechanism at the atomistic level to assist in scale-up on an industrial scale.

Molecular simulation is employed to elucidate the sorption process and has emerged as a rising novel technology due to its undeniable advantages. Molecular dynamics simulations provide a platform for understanding molecular-level interactions and atomistic structures. In addition, entirely new or modified adsorbents can be discovered from a well-defined simulation environment. In a recent work by Jimenez et al. (2021) [13], they studied the interaction between metallic ions and adsorbents with an oxygen-containing group (e.g., OH) to understand the adsorption process for impurities removal from water. In their work, they reported a strong attraction towards that group with a small bond distance, which aided in the adsorption of metal contaminants on the adsorbent surface. The adsorption process was observed using a sorption module while calculating the sorption loading. The molecular structures were required to be optimized prior to the calculation of sorption loading [14] using simulation software, which could be further used in predicting the adsorption capacity of the new generation materials.

It was found that although a myriad of experimental and simulation work has been available to study the adsorption phenomenon, a comprehensive study of molecular simulation for the adsorption process using different adsorbents is scarcely available for wastewater treatment covering different contaminants and pollutants. There should be comprehensive literature related to molecular simulation studies for wastewater treatment using different adsorbents, as this would allow scholars to select the best adsorbent for corresponding contaminants with an excellent and effective adsorption capacity. In this paper, we reviewed simulation studies of different adsorbents that were categorized into (1) carbon-based, (2) oxides and hydroxides, (3) zeolites, (4) metal–organic frameworks and (5) clay. These are the most conventionally used adsorbents for various wastewater treatment applications. These adsorbents and their accompanied simulation study were critically reviewed, and future perspectives for this study were also highlighted. Comparing values with experimental or theoretical calculations for these adsorbents proved that molecular dynamic simulation is a successful research tool and can lead to optimal wastewater treatment. Most of the authors have compared their computational results with

experimental results for their work, i.e., Mohammed et al. (2019), Galdino et al. (2021), Jim'enez et al. (2021), Liu et al. (2021), Han et al. (2022), Tuzen et al. (2022), Chang et al. (2020), Dhar et al. (2021), Dryaz et al. (2021), Firouzjaei et al. (2020), Han et al. (2022), Zhang et al. (2021) and Li et al. (2021), suggesting a good agreement of experimental values with computational findings. The suitability and pertinency of various approaches for estimating the adsorption capacity for different adsorbents is also reported herein.

2. Molecular Simulation and Application in Adsorption Study

Molecular dynamic simulations uncover the various aspects that affect the adsorption process, such as the electrostatic interaction, binding energy, Gibbs free energy, adsorption energy and loading value. All these factors were illustrated in Figure 1. The binding energy affects the molecules' structural stability [15], whereby the negative value of the binding energy shows that the structure is stable. Zhang et al. (2018) [16] studied the interaction at the molecular level to understand the mechanism of graphene oxide for the adsorption process of aromatic compounds. The π-π interaction was defined for geometrically optimized molecular structures and adsorption energies were calculated. The higher the adsorption energy, the more the adsorption capacity and hence the better the adsorbent. A simulation study discussing Gibbs free energy was also conducted to help in understanding the adsorption process by indicating the thermodynamic feasible interaction of the adsorbent with sorbate [17]. The negative value of Gibbs free energy indicated the spontaneous reaction, which demonstrated feasibility for the adsorbent to sorb pollutant.
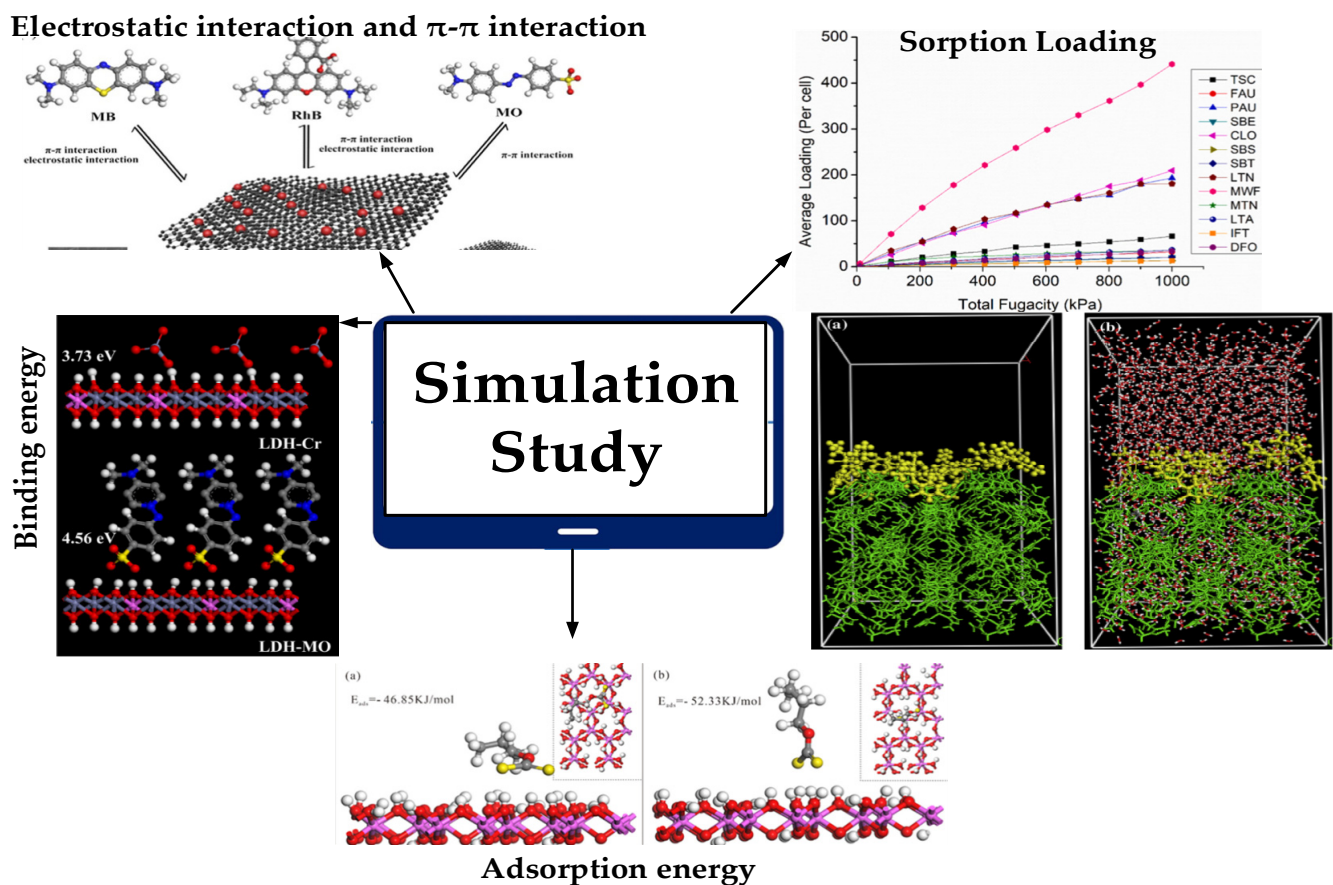

Figure 1. Illustration of study variables for adsorption using molecular simulation. Reprinted with permission from Ref. [18] Copyright 2019 Elsevier, Abdelhameed et al., 2019. Reprinted with permission

from Ref. [19] Copyright 2020 Elsevier, Chang et al., 2020. Reprinted with permission from Ref. [20] Copyright 2018 Elsevier, Meng et al., 2018. Reproduced with permission from Ref. [21] Copyright 2021 Elsevier, Zhang et al., 2021. Reprinted with permission from Ref. [14] Copyright 2021 Elsevier, Wanyonyi et al., 2021.

The equations used to calculate the adsorption energy and interaction energy are provided in Equations (1) and (2), respectively:

$$E_{ads} = E_1 - E_2 - E_3 \tag{1}$$

In Equation (1), E_1 represents the energy of a complex comprising the adsorbent + contaminant while E_2 and E_3 correspond to the energy of the isolated adsorbent and contaminant, respectively:

$$V_{ij} = V_{LJ} + V_C \tag{2}$$

For Equation (2), V_{ij} depicts the interaction energy while V_{LJ} represents the energy that was dependent upon the distance between atoms and V_C, the energy obtained by the electrostatic conversion factor.

Different types of simulation software, such as Gromacs 5.0.2 software [22], HyperChem 8 software [17], Materials Studio (MS) software [5,13,17–24], Gaussian 09 software [25,26], Tera-Chem software [27] and LAMMPS software [24] were used for the molecular dynamics simulation (MDS) study. Most studies were based on the Monte Carlo simulation approach [20,28] and density functional theory (DFT) [20,29]. The Monte Carlo Simulation (MCS) approach was a collection of different methods including configurational bias simulation in which the adsorption of sorbate molecules was observed when the sorbate molecule fitted the pores of the framework without steric overlap [30]. Particularly, the Metropolis Monte Carlo was used during MCS in which the adsorption of sorbate molecules was observed by their positions and orientations while the sorbent was treated as a rigid body [31]. The Grand Monte Carlo Simulation (GMCS) approach was used to prognosticate the adsorption of pollutants on the adsorbent. A grand canonical simulation approach allows the number of molecules or particles to change, providing a convenient way to perform simulation calculations where the system is altered by external conditions [32]. By performing these calculations, adsorption isotherms were obtained and the shape of the isotherms indicated the adsorbent's behavior for the pollutant [32].

On the other hand, the DFT calculations stated that all ground-state properties were a function of the charge density, ρ, and the total energy, E_t (kcal/mol) [33]. Different modules could be employed using DFT, in which molecular structures were optimized and adsorption energy calculations were performed to estimate adsorption during the process. For this purpose, the geometry optimization of molecular structures was initially performed to obtain the most stable structure, followed by the application of the electronic distribution density method to manipulate the charge transfer and then a molecular dynamic simulation to analyze the thermal stability that assisted in calculating the energy values for adsorption capacity estimation [34]. The molecular simulation showed great potential to predetermine the adsorption capacity of the adsorbent before proceeding with the actual process, which was costly and time-consuming to be realized from experimental interrogation [35]. Moreover, the molecular dynamic simulation provided a platform where the adsorption phenomenon was studied microscopically within a sufficient time period, economical means, and space. To date, molecular simulation is regarded as a successful research tool to explicate the adsorption process [13,32].

2.1. Carbon-Based

Carbon-based adsorbents are widely used in water and wastewater treatment as they are abundant and have good efficiency to adsorb pollutants from water [33,34]. Moreover,

carbon-based compounds have great thermal stability and a good adsorption capacity [8]. Molecular simulation studies of carbon-based adsorption separation are given in Table 1.

It was observed that the adsorption capacity could be estimated, and the adsorption process was understood using the molecular interaction energy. With simulation calculations, the interaction energy for methylene blue adsorption on the Bituminous Coal surface was calculated to be −122.28 kJ/mol [36], suggesting a spontaneous interaction of MB with the carbon-based adsorbent. In addition, the molecular simulation illustrated that the MB molecules' attraction with the water molecules was due to hydrogen bonding and the negative value of ΔG^0 was in agreement with the spontaneous adsorption simulation results. The adsorption process was discovered to be affected by the electrostatic field, the pore size of the adsorbent and ultrasound waves. In a simulation study for phenol adsorption [22], it was observed that the increase in the electrostatic field enhanced the interaction energy to promote adsorption, i.e., the Van der Waals energy of C-P was −1571.21 kJ/mol under zero electrostatic field. In Figure 2a, it was seen that when there was no electrostatic field (on the left side), the Van der Waal energy was around −1500 kJ/mol, and when a 3 V/nm electrostatic field was applied, it was increased to around −1700 kJ/mol. In Figure 2b, the graphs show that when the electrostatic field strengths were increased to 1 V/nm, 2 V/nm, 3 V/nm, 4 V/nm and 5 V/nm, the values of the Van der Waals energy (VLJ) were improved (which enhanced the adsorption capacity) by −1701.38 ± 11 kJ/mol, −1768.63 ± 11 kJ/mol, −1785.83 ± 11 kJ/mol, −1798.96 ± 11 kJ/mol and −1803.04 ± 11 kJ/mol, respectively. The effect of the pore size and adsorbent concentration on the adsorption process were understood using a simulation study for phenol removal via activated carbon by Galdino et al. (2021) [37], where different carbon with varying pore sizes (e.g., 8.9, 18.5 and 27.9 Å) were simulated to observe the isotherms. It was reported that at a low concentration, a pore size of 8.9 Å was the most efficient in removing diluted phenol in water. Moreover, a smaller pore size enhanced filling, resulting in efficient adsorption [37]. Thermodynamic parameters also played a significant role in adsorption capacity, which could be influenced by the electrostatic field and ultrasound waves as they would promote a molecular interaction that enhanced the sorption ability.
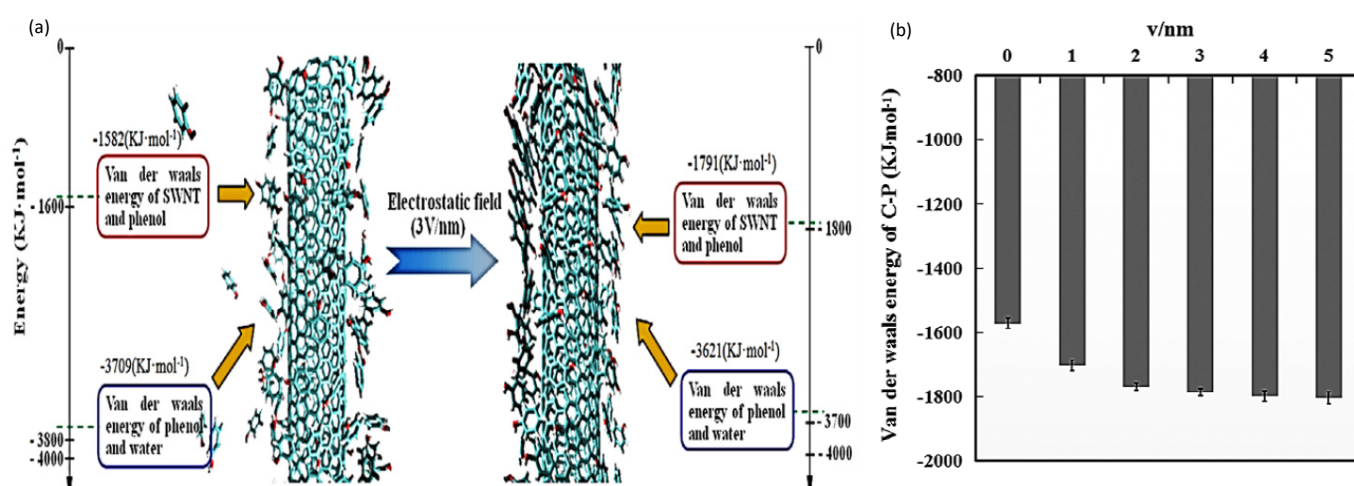

Figure 2. Effect of electrostatic field on adsorption process for phenol removal using single-walled carbon nanotubes (**a**) The electrostatic field promoted the adsorption of phenol on single-walled carbon nanotubes; (**b**) the electrostatic field strengths and the respective values of Van der Waal energy in kJ/mol. Reprinted with permission from Ref. [22] Copyright 2019 Elsevier (Zhang et al., 2019).

Table 1. Molecular simulation studies of carbon-based adsorption separation.

Adsorbent	Study Domain	Simulation Environment Operating Conditions	Surface Area (m²/g)	Simulation Result	Adsorption Capacity (mg/g)	References
Single-walled carbon nanotubes	A molecular dynamics simulation study for adsorption of phenol on single-walled carbon nanotubes under the influence of electrostatic field.	• Temp: 298 K • Pressure: 1.01 × 10⁵ Pa	NA	The electrostatic field strengths and the value of Van der Waal energies in kJ/mol were: • 0 V/nm: −1571.21 ± 11 KJ/mol • 1 V/nm: −1701.38 ± 11 KJ/mol • 2 V/nm: −1768.63 ± 11 KJ/mol • 3 V/nm: −1785.83 ± 11 KJ/mol • 4 V/nm: −1798.96± 11 KJ/mol • 5 V/nm: −1803.04 ± 11 KJ/mol	NA	Zhang et al. (2019) [22]
Bituminous Coal	Adsorption mechanism and molecular simulation for methylene blue (MB) adsorption on Bituminous Coal.	298 K.	NA	• Interaction energy between the coal surface and MB was determined to be −122.28 kJ/mol. • MS showed that MB molecules attracted the water molecules due to hydrogen bonding.	NA	Huang et al. (2019) [36]
Activated carbon	Estimation of the phenol adsorption on activated carbon by pore methodology.	301 K	NA	• The smaller the pore, the sooner the filling occurred. • Presence of 8.9 Å pores was essential to adsorption even in very low phenol concentrations.	Max. adsorption capacity; • Maxsorb: 1300 • PC76: 900, PC58: 700 • WV1050: 550 • Norit-RB4: 349	Galdino et al. (2021) [37]

Bituminous activated carbon (BAC), bone char (BC), iron modified activated carbon (FeC), coconut shell activated carbon (CC), manganese modified zeolite (KL), natural zeolite (NZ) and silica (S)	Removal of impurities from nickel-plating baths by adsorption on commercial sorbents to reduce wastewater discharges.	• Temp: 25 °C
		• Pressure: 1 atm
			NA	• Both OH- and PO₄ groups of Hap were responsible for the electrostatic interaction with the metallic species.
				• Values of ion–oxygen distance (IOD) were:
				  ○ Ni²⁺ 1.96
				  ○ Zn²⁺ 1.98
				  ○ Ca²⁺ 2.58
				  ○ K⁺ 2.48
					The adsorption capacity of Zn²⁺:
					• 16.97 at 30 °C
					• 29.51 at 60 °C.
						Jiménez et al. (2021) [13].

Table 1. *Cont.*

Adsorbent	Study Domain	Simulation Environment Operating Conditions	Surface Area (m²/g)	Simulation Result	Adsorption Capacity (mg/g)	References
Lignite (Coal)	To understand adsorption phenomenon of ammonia nitrogen and phenol onto lignite surface using experimental and molecular dynamics simulation study.	298 K	7.102	Adsorption energies in kcal/mol were: • Absorbent NH_4-N (no phenol): −210.62 • NH_4-N (presence of phenol): −201.16 • phenol (absence of NH_4-N): −172.56 • phenol (presence of NH_4-N): −226.25	NA	Liu et al. (2021) [26].
Single-walled carbon	A study by molecular dynamics simulation and experiment for influence of ultrasound on the adsorption of single-walled carbon nanotubes to phenol	300 K	NA	For ultrasound with frequencies, the values of Van der Waals energies of SWNTs-phenol in kJ/mol were: • 200 MHz: −1587.39 • 250 MHz: −1530.6 • 333 MHz: −1473.58 • 500 MHz: −1446.23 • 1000 MHz: −1268.59.	NA	Han et al. (2022) [38].
Activated carbon (AC) with diethylenetriamine (DETA)-trimesoyl chloride (TMC) copolymer	Theoretical and experimental analyses for synthesis of carbon modified with polymer of diethylenetriamine and trimesoyl chloride for the dual removal of Hg (II) and methyl mercury ([CH_3Hg]+) from wastewater.	NA	NA	Calculated adsorption energies (E_a) in kcal/mol were: • DETA-TMC: 0.79 • DETA-TMC-AC: 2.40 • [CH_3Hg]+ on DETA-TMC-AC: 1.07 • $Hg2+$ on DETA-TMC-AC: 15.55	The adsorption capacity of developed composite: • 317.3 for Hg(II) • 263.6 for CH_3Hg+	Tuzen et al. (2022) [27]

2.2. Oxides and Hydroxides

Oxides and hydroxides are classified as good adsorbents because of their excellent adsorption capacity. Compounds such as graphene oxide and its derivatives are primarily used for wastewater treatment [19], while double-layered hydroxides have various remarkable applications in the field of wastewater treatment due to their excellent adsorption ability [36,39]. Graphene oxide and its derivatives have recently caught much attention due to their unique physicochemical properties [16]. Graphene oxide has been declared as the most promising nano-adsorbent for water treatment so far [28], which is used mostly for organics removal from wastewater [16,40] Double-layered hydroxides have attracted significant attention in recent years [41] and have been recognized as good adsorbents because of their high surface area and ion exchangeability [36,39]. A combination of double-layered hydroxide and graphene oxide was also introduced for wastewater treatment, which demonstrated a remarkably excellent adsorption capacity for the removal of dye pollution from wastewater [42]. Another attractive class of oxides and hydroxides is functionalized mesoporous silica, considered one of the best adsorbents due to its high adsorption performance and well-organized pore system [17,18].

The simulation studies using these adsorbents for wastewater treatment were comprehended and are summarized in Table 2.

It was found that the Gibbs free energy, binding energy and adsorption energy helped in determining the adsorption capacity of the adsorbent. Delgadillo-Velasco et al. (2018) [17] studied the adsorption of phosphates on various adsorbents including classes of oxides and hydroxides, which were proven to be the best adsorbent for phosphate removal from water with a maximum adsorption capacity of 193.75 mg/g at pH 7 in comparison to natural zeolite and silica with adsorption values of only 2.92 and 4.17 mg/g, respectively. Moreover, the Gibbs free energy of −21.38 kcal/mol revealed that it was possible to recover the phosphates and reuse them later. This simulation study could help in future research to understand the recovery of metal elements after the adsorption process. The class of oxides and hydroxides achieved the maximum value of −21.38 kcal/mol.

Meng et al. (2018) [20] studied the binding energy and interaction of adsorbents for the removal of methyl orange and Cr anionic contaminants from mixed wastewater by Zn-Al layered double hydroxides. They found that the negative charge part of the contaminant was very close to the LDH layers and reaffirmed the interaction between OH and LDH. Moreover, the binding energy between the ZnAl-LDH layer and MO was more than the binding energy between the ZnAl-LDH layer and Cr, e.g., 4.56 eV versus 3.73 eV. So, methyl orange had a stronger affinity than Cr for ZnAl-LDH layers. Cao et al. (2021) [43] and Pelalak et al. (2021) [25] determined adsorption energies for the estimation of the adsorption capacity in the removal of dyes (TAF/MPS-water-RB and TAF/MPS-water-NR) using amino-functionalized silica, which was simulated to be −211.8159 and −4.8448 kcal/mol, respectively [43]. So, for the removal of cationic dyes, TAF/MPS (3-Trimethoxysilylpropyl) with a diethylenetriamine linker was proven to be an efficient adsorbent. The latter also studied functionalized meso-silica for the adsorption of different pollutants in wastewater, and calculated the adsorption energy with a simulation study, which was obtained at −113.92, −247.00 and −166.01 kcal/mol for MPS-linker-water-NR, MPS-linker-water-CV and MPS-linker-water-OII, respectively. The adsorption energy of MPS-linker-water-NR was less negative than that of MPS-linker-water-CV and MPS-linker-water-OII.

Table 2. Simulation studies using oxides and hydroxides for wastewater treatment.

Adsorbent	Study Domain	Simulation Environment Operating Conditions	Surface Area (m²/g)	Simulation Result	Adsorption Capacity (mg/g)	References
Activated carbon, bone-char, catalytic carbon, natural-silica, natural-zeolite, manganese(II) oxide-composite, iron(III)hydroxide	A molecular simulation modeling for screening of different commercial sorbents for the removal of phosphates from water.	• Temp: 30 °C. • pH: 2–7	• NaH_2PO_4: 213.13 • $Fe(OH)_3$: 209.90 • Complex $NaH_2PO_4.Fe(OH)_3$-H_2O: 644.96	Gibbs free energy in kcal/mol was: • NaH_2PO_4: 0.3654 • $Fe(OH)_3$: −0.022 • Complex $NaH_2PO_4.Fe(OH)_3$-H_2O: −21.3887	$Fe(OH)_3$ had the higher adsorption capacity of: • 194 at pH 7 • 323 at pH 2	Delgadillo-Velasco et al. (2018) [17].
0Zn-Al layered double hydroxides (ZnAl-LDH)	Adsorption of methyl orange and Cr anionic contaminants (present in wastewater) by in situ formation of Zn-Al layered double hydroxides.	• 298 K	NA	The binding energies in eV were: • ZnAl-LDH layer and MO was 4.56 eV • ZnAl-LDH layer and Cr was 3.73 eV	NA	Meng et al. (2018) [20].
Graphene oxide (GO)	Understanding the molecular interlinkage between graphene oxide and aromatic organic compounds with implications on wastewater treatment.	• pH: 2 to 5.6	NA	Adsorption energies E_{ad} in kcal mol^{-1} were: • MB/graphene: 0.28 • MB/epoxy-graphene: −0.96 • MB/unionizedcarboxyl-graphene: −0.07 • MB/ionized carboxyl graphene: −2.44	NA	Zhang et al. (2019) [16].
Magnetic $CoFe_2O_4$/graphene oxide	Experimental and molecular dynamics simulation study for high-efficiency and selective adsorption of organic pollutants on magnetic $CoFe_2O_4$/graphene oxides.	(298 K).	NA	Adsorption energies in kcal/mol were: • GO + MB −1.523 • GO + RhB −1.505 • GO + MO −0.209 • DGO + MB −1.565 • DGO + RhB −1.519 • DGO + MO −0.214	The maximum adsorption capacity from Langmuir equation were: • MB: 355.9 • RhB: 284.9 • MO: 53.0	Chang et al. (2020) [19].

Table 2. *Cont.*

Adsorbent	Study Domain	Simulation Environment Operating Conditions	Surface Area (m²/g)	Simulation Result	Adsorption Capacity (mg/g)	References
MFe_2O_4@GO	Removal of dye by metal ferrite-enabled graphene oxide nanocomposites using adsorption.	• $NiFe_2O_4$@GO: 298.15 K, 318.15 K, 328.15 K. • $CuFe_2O_4$@GO: 298.15 K, 318.15 K, 328.15 K.	NA	(1) The enthalpy energies of the adsorption reaction in kcal/mol were: • $NiFe_2O_4$@GO: 15.16 • $CoFe_2O_4$@GO: 12.00 • $CuFe_2O_4$@GO: 12.66 (2) The entropies in (J/mol K) were: • $NiFe_2O_4$@GO: 110 • $CoFe_2O_4$@GO: 93 • $CuFe_2O_4$@GO: 100	The adsorption capacity of varying GO nanocomposites were: • $NiFe_2O_4$@GO: 76.34 • $CoFe_2O_4$@GO: 50.15 • $CuFe_2O_4$@GO: 25.81	Bayantong et al. (2021) [1].
Amino-functionalized silica	Understanding adsorption process using molecular dynamic simulations and quantum chemical calculations for wastewater treatment using amino-functionalized silica.	NA	NA	Adsorption energies in kcal/mol were: • MPS-water-RB: −162.3930 • MPS-water-NR: −2.9360 • TAF/MPS-water-RB: −211.8159 • TAF/MPS-water-NR: −4.8448	NA	Cao et al. (2021) [43]
Graphene Oxide Shielded Mg−Al-Layered Double Hydroxide	Methylene blue removal by Graphene Oxide Shielded Mg−Al-Layered Double Hydroxide from synthetic wastewater using adsorption.	298 K	NA	Strong nonbonding interactions were observed as follows: • C−H⋯O (2.66–2.77 Å) • pi-donor⋯H−O (2.89–3.05 Å) • and S⋯H−O (2.28 Å)	The maximum adsorption capacity was: • 0.5 mmol/g for Mg−Al-LDH • 0.85 mmol/g for modified Mg−Al-LDH with GO	Dhar et al. (2021) [42].
Graphene oxide-chloroacetic acid	Molecular dynamics simulation study for lead removal using adsorption of graphene oxide with chloroacetic acid (to increase the potentiality of GO)	298 K	NA	Total energies of GO layers in kJ/mol were: GO: Pb^{+2} vs. energy values • 1:25:5094.19 • 1:50:15,836.50 • 1:100:36,423.75	According to the Langmuir isotherm, maximum adsorption capacities (qe) were: • GO 0.25 mol/g • GO/CAA 0.52 mol/g	Hossain et al. (2021) [28]

Table 2. *Cont.*

Adsorbent	Study Domain	Simulation Environment Operating Conditions	Surface Area (m²/g)	Simulation Result	Adsorption Capacity (mg/g)	References
Multilayer graphene oxide	An experimental and molecular dynamics simulation study for xanthate removal from aqueous solution by multilayer graphene oxides adsorbent.	Simulation at two stages. • Constant pressure–temperature (NPT) • Temperature was 298.15 K	NA	As the simulation progressed from time 250 ps to time 750 ps, the xanthate molecules gradually deformed, which showed a tendency to be gradually adsorbed on the MGO surface.	NA	Li et al. (2021) [40].
Diamino-functionalized hollow mesosilica spheres	Molecular dynamics simulation for dye removal from synthetic wastewater using novel diamino-functionalized hollow mesosilica spheres.	NA	NA	The adsorption energy in kcal/mol after optimization were: • DAF-HMSS-CV-water: −269.3617 • DAF-HMSS-NR-water: −130.6799	NA	Pelalak et al. (2021) [23].
Functionalized Meso-silica	A molecular dynamics simulation for removal of different pollutants using functionalized mesosilica adsorbent.	NA	NA	Adsorption energy in kcal/mol were: • MPS-linker-water-NR: −113.92 • MPS-linker-water-CV: −247.00 • MPS-linker-water-OII: −166.01	NA	Pelalak et al. (2021) [25].

A molecular simulation helped determine the adsorption sites and indicated how adsorption increased with the introduction of other compounds and elements, i.e., the introduction of the GO layers into the LDH structure. The interaction energy represented the stability of the sorption system, with the more negative value having more stability. Chang et al. (2019) [19] systematically calculated adsorption energies to investigate the interaction of dye molecules with graphene oxide (GO) in a study of organic pollutants removal by a magnetic $CoFe_2O_4$/graphene oxide adsorbent. The negative interaction energy between the dye and the GO model suggested greater stability of the adsorption system, in which the calculated adsorption order of GO with the three dyes was MB > RhB > MO at −1.523, −1.505, and −0.209, respectively. Dhar [42] also studied the interaction of methylene blue (MB) with graphene oxide (GO) layers and observed a significant attraction between the MB molecules and GO layers of the composite. Dhar found three major interactions in the simulation environment as shown in the Figure 3, in which the hydrogen bonding interaction, pi donor interaction and non-bonding interaction in between oxygen and sulfur were clearly observed. The values of these interacting distances were 2.49–3.04 Å for the nonclassical hydrogen bonds between hydrogen and oxygen C−H···O, 2.45–3.00 Å for the pi-donor interaction H−O and 3.29 Å for the non-bonding interaction between sulfur···oxygen.
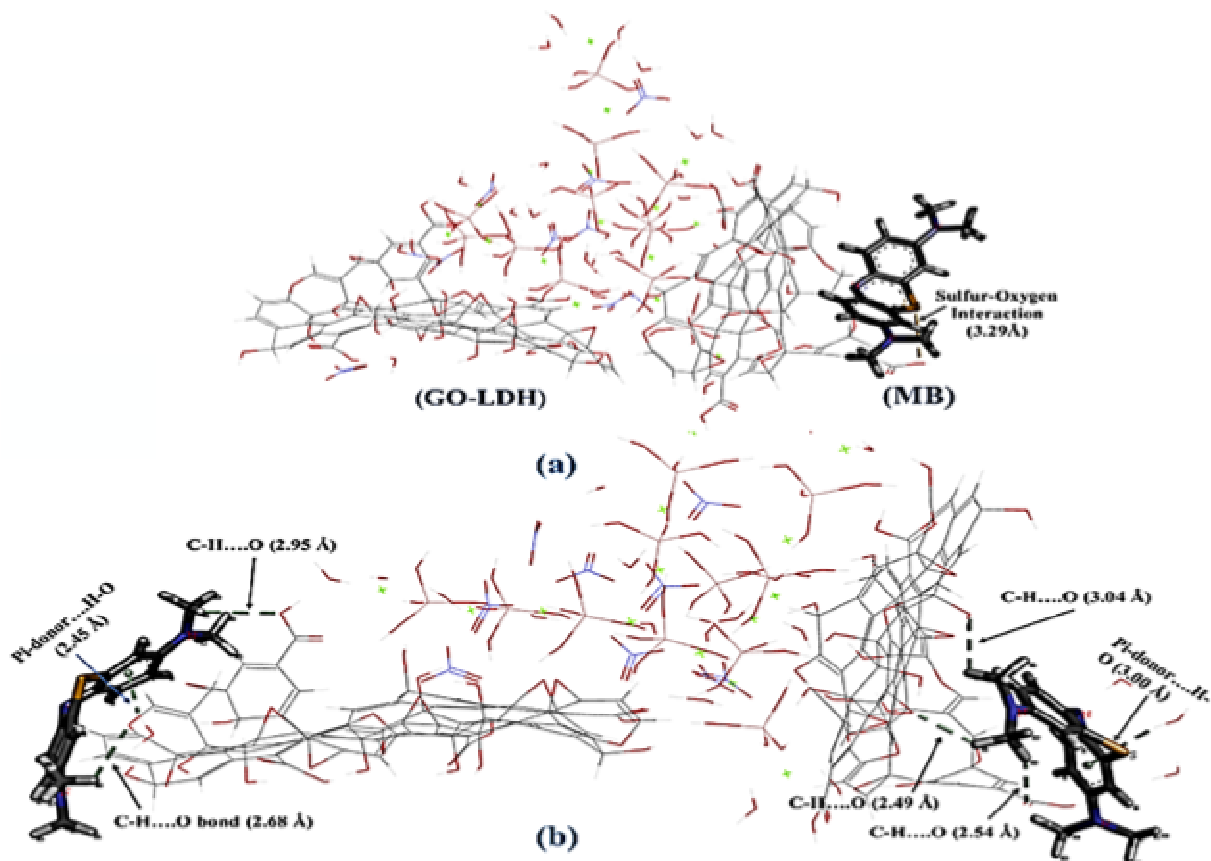

Figure 3. Illustration of MB and GO-LDH bonding and nonbonding interaction in simulation environment. Two products are seen: (**a**) one MB molecule on one GO layer; (**b**) two MB molecules on both GO layers. Reproduced with permission from Ref. [42] Copyright 2021 Elsevier, Dhar et al., 2022.

2.3. Zeolites

Zeolite compounds are regarded as a unique and distinct class of adsorbents due to their ion exchangeability and well-defined structures [3,40,44]. These compounds are mostly used for environmental applications and also in the field of wastewater treatment

because of their low cost and high surface area. The simulation studies using different zeolites for wastewater treatment are summarized in Table 3.

The simulation study for different zeolites revealed that the adsorbent's structure and surface-to-volume ratio played a significant role in the adsorption process. Bedneezad et al. (2019) [3] studied the adsorption of methylene blue dye on natural clinoptilolite and clinoptilolite modified by iron oxide nanoparticles and concluded that effective adsorption happened as a result of the high surface-to-volume ratio of the modified adsorbent as well as the density of the functional groups. In a simulation study for the adsorption of Cu^{2+}, Cd^{2+} and Pb^{2+} ions on different sodium-based zeolites [24], it was found that different zeolites have varying tendencies to adsorb them. The LTA/Na zeolite showed the highest adsorbed ions of 69% while the FAU structure showed the lowest with 46% for cadmium adsorption. For Pb^{2+}, LTA also had maximum adsorbed ions of 53%. On the other hand, for the Cd ion adsorption, the EDI zeolite showed a good percentage with 61%. Different zeolites had different tendencies to attract different ions or pollutants; similarly, different zeolites were elucidated to have different adsorption performances at varying temperatures. Mohammed et al. (2019) [5] performed a simulation study for a faujasite-type Y zeolite at three different temperatures of 293, 303 and 313 K. It was found that the phenol adsorption decreased (84, 82 and 80 mg/g, respectively) with greater temperature due to increased entropy.

Table 3. The simulation studies using different zeolites for wastewater treatment.

Adsorbent	Study Domain	Simulation Environment Operating Conditions	Surface Area (m²/g)	Simulation Result	Adsorption Capacity	References
Clinoptilolite	Adsorption of methylene blue dye from wastewater using natural clinoptilolite and clinoptilolite modified by iron oxide nanoparticles.	pH 2–10	NA	Effective adsorption because of high surface-to-volume ratio of the modified adsorbent as well as the density of the functional groups at the surface of the adsorbent.	NA	Badeenezhad et al. (2019) [3]
FLTA, FAU, EDI, THO, NAT and LTN zeolites	Molecular simulation study for adsorption mechanism of Cu^{2+}, Cd^{2+} and Pb^{2+} ions on different zeolites exchanged with sodium.	Temp 298 K	NA	The cadmium adsorptions in % were: • LTA/Na zeolite:69% (highest) • FAU:46% (lowest)	NA	Khanmohammadi et al. (2019) [24].
Faujasite-type Y zeolite (NaY)	Adsorption isotherms, kinetics and grand canonical Monte Carlo simulation studies for adsorption of phenol on faujasite-type Y zeolite	• Range of temperatures: (293, 303 and 313 K)	558.75	The phenol uptakes of zeolite in mg/g were: • At 293 K: 84 • At 303 K: 82 • At 313 K: 80	The phenol uptakes of zeolite in mg/g were: • At 293 K: 84 • At 303 K: 82 • At 313 K: 80	Mohammed et al. (2019) [5].
High-silica Zeolite	An experimental and Monte Carlo simulation study for adsorption mechanisms of organic micropollutants on high-silica-zeolites causing S-shaped adsorption isotherms	NA	NA	The adsorption loadings of TCP were: • FAU250: 1700 • FAU50: 1300 • FAU40: 1150	NA	Jiang et al. (2020) [45].
X- and Y-type faujasite zeolites	A computational study for phosphate removal from wastewater using faujasites.	NA	NA	• Terminal hydrogen atoms of zeolites were found at a distance of 0.97 Å from the oxygen atoms. • This value increased to 1.1 Å for hydroxides interacting with phosphate.	NA	Capa-Cabos et al. (2021) [46].

Table 3. *Cont.*

Adsorbent	Study Domain	Simulation Environment Operating Conditions	Surface Area (m²/g)	Simulation Result	Adsorption Capacity	References
Padina gymnospora/zeolite nanocomposite	Design, characterization and adsorption properties of Padina gymnospora/zeolite nanocomposite for removal of Congo red dye from wastewater	NA	• Z: 91.2 • PG: 126.7 • ZPG: 117.3	Adsorption energies (kcal/mol) of Congo red adsorbed on zeolite clinoptilolite with 3, 5 and 7 nm simple box systems: • 3: −42.22350 • 5: −40.83882 • 7: −38.15356	The adsorption capacities were: • ZPG: 11.26 • PG: 11.59 • Z: 8.0	Dryaz et al. (2021) [29].
Zeolite framework	Role of pore chemistry and topology for heavy metal removal using zeolite (a molecular simulation to machine learning).	NA	NA	Loadings of Cr (VI) ions were: • TSC: 5, FAU: 3 • PAU: 6, SBE: 1 • CLO: 21, SBS: 1 • SBT: 2, LTN: 7 • MWF: 12, MTN: 1 • LTA: 3, ITV: 2 • IFT: 3, DFO: 3	NA	Wanyonyi et al.(2021) [14]

The size of the adsorbent also played a significant role in the adsorption process. Dryaz et al. (2021) [29] demonstrated in their study that the adsorption energy was affected by the size of the adsorbent. It was observed that for red dye adsorption on zeolite clinoptilolite, the size of the adsorbent simulation cell affected the adsorption energy value, in which an increase in the size of the box decreased the value. Three simple boxes of size 3 nm, 5 nm and 7 nm were selected, and 3 nm and 7 nm are shown in Figure 4, whereby the interacting distance between the atoms were observed to be increasing and the adsorption energy value decreased. The adsorption energy values were obtained at −42.22350801, −40.83882700 and −38.15356471 kcal/mol, respectively. Another factor that affected the adsorption process was the electrostatic interaction, which helped to promote the adsorption phenomenon. Capa-Cabos et al. (2021) [46] studied this for the adsorption of phosphate pollutant on a faujasites zeolite. They found that the electrostatic interaction of the ions and oxygen atom from the zeolite promoted adsorption via the change in hydrogen atoms arrangement. In the heavy metal sorption by zeolites, the sorption isotherms were studied [14], and the loading per cell indicated the adsorption capacity. The loading value of the lead ions on zeolite was determined and a maximum loading value of 728 was obtained for the CLO zeolite framework while MWF showed maximum loading for the Cadmium ion with a loading value of 450. Hence, every zeolite had a different tendency to sorb various contaminants.
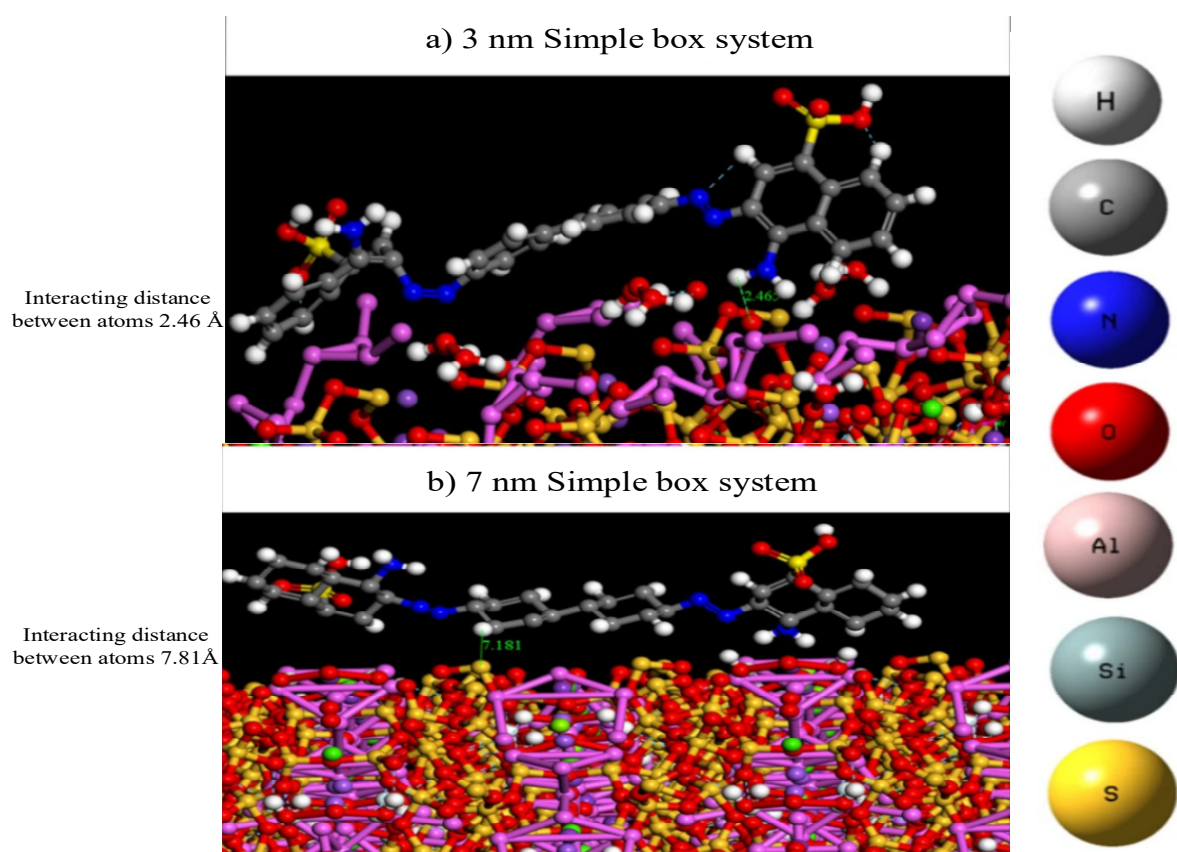

Figure 4. Illustration of different sizes simple box of (**a**) 3 nm and (**b**) 7 nm for adsorption study using zeolites in simulation environment.

2.4. Metal–Organic Framework

A new class of hybrid material used for different applications of separation and purification is the metal–organic framework [21,45,47]. Their exceptional good qualities, which include low density and big pore size, have attracted a notable amount of attention among various classes of adsorbents [48] The simulation studies using different metal–organic frameworks for wastewater treatment are given in Table 4.

Table 4. The simulation studies using different metal organic frame for wastewater treatment.

Adsorbent	Study Domain	Simulation Environment Operating Conditions	Surface Area (m²/g)	Simulation Result	Adsorption Capacity (mg/g)	References
Zeolitic imidazolate frameworks	Experimental and molecular simulation studies for efficient removal of pesticides from wastewater using Zeolitic imidazolate frameworks	298 K	NA	The maximum loadings of pesticides were: • Prothiofos on ZIF-8: 14 • Ethion on ZIF-18: 11 • Prothiofos on ZIF-67: 10 • Ethion on ZIF-67: 9	Adsorption capacity of pesticides were: • Prothiofos on ZIF-8: 366.7 • Ethion on ZIF-8: 279.3 • Prothiofos on ZIF-67: 261.1 • Ethion on ZIF-67: 210.8	Abdelhameed et al. (2019) [18]
Various metal organic frameworks; MIL-101(Cr), MIL-100(Cr), Cu-BTC, DUT-23(Cu), UIO-66 and UMCM-2	The adsorption and diffusion properties of Terephthalic Acid for different metal organic frameworks was studied using molecular simulation.	298 K	• MIL-101(Cr): 3284.80 • MIL-100(Cr): 2147.14 • Cu-BTC: 1997.20 • DUT-23(Cu): 4758.42 • UIO-66: 799.59 • UMCM-2: 4361.05	TPA adsorption in mg/g were: • UMCM-2: 1894.19 • UIO-66: 199.67	The TPA adsorption capacities were: • UMCM-2: 1894.19 • UIO-66: 199.67	Bigdeli et al. (2019) [49].
U iO-66(Zr).	The application of experimental and molecular simulation method for extraction of androgens and progestogens in environmental water samples using UiO-66(Zr) as sorbent.	NA	NA	• UiO-66(Zr) exhibited more significant binding ability of −7.96 to −9.94 kcal/mol towards the analytes • It was greater than other three MOFs {MIL-101(Cr), MIL-100(Fe), MIL-53(Al)} • UiO-66(Zr) was more suitable to be a sorbent for adsorption of androgens and progestogens.	NA	Gao et al. (2019) [48].
Graphene oxide-copper-metal organic framework nanocomposite	Experimental and molecular dynamics study for adsorption of dye from water using a graphene oxide-copper-metal organic framework nanocomposite.	• Annealing cycles with an initial temperature of 300 °C • Midcycle temperature of 500 °C.	NA	Adsorption energies in kcal/mol were: • GO-Cu-MOF: −323 • Cu-MOF: −119	Adsorption capacity of GO-Cu-MOF at different temperatures was: • 25 °C: 173 • 45 °C: 251 • 65 °C: 262	Firouzjaei et al. (2020) [50].

Table 4. *Cont.*

Adsorbent	Study Domain	Simulation Environment Operating Conditions	Surface Area (m²/g)	Simulation Result	Adsorption Capacity (mg/g)	References
Amino-functionalized Al-MIL-53	Molecular dynamic study for intermolecular interactions of dimethoate pesticide on amino-functionalized Al-MIL-53	NA	• Al-BDC: 866 • [Al-(BDC) 0.75(BDC-NH2)0.25]: 1105 • [Al-(BDC) 0.5(BD-CNH2)0.5]:1260 • [Al-(BDC) 0.25(BDC-NH2)0.75]: 1100 • Al-BDC-NH$_2$: 1060	The adsorption energies of dimethoate onto Al-MOFs in kcal/mol were: • Al-BDC: -29.5 • Al-(BDC)0.75(BDC-NH2)0.25: -30.1 • Al-(BDC)0.5 (BDC-NH2)0.50: -30.1 • Al-(BDC)0.25(BDC-NH2)0.75: -31.1 • Al-BDC-NH2: -31.4	Pesticide adsorption capacities were: • Al-BDC: 154.8 • [Al-(BDC)0.75(BDC-NH2)0.25]: 267.2 • [Al-(BDC) 0.5(BDC-NH2)0.5]: 513.4 • [Al-(BDC) 0.25(BDC-NH2)0.75]: 344.7 • Al-BDC-NH2: 266.9	Abdelhameed et al. (2021) [51].
Zeolitic imidazolate frameworks	A molecular simulation study for Zeolitic imidazolate frameworks as capacitive deionization electrodes for water desalination and Cr(VI) adsorption	300 K	NA	CdIF-1 (96.5%) has the second highest average R-value despite having the highest average water flux R-value (0.0308 Å/ns)	NA	Hong et al. (2021) [52].
Metalorganic nanotube sponge	Experiment and molecular simulation study for fabrication of thermoresponsive metalorganic nanotube sponge and its adsorption of endocrine-disrupting compounds and pharmaceuticals/personal care products	303 K	137	Adsorption energy () of DBP and PCMX on different crystal surfaces in kcal/mol were: • Cu-MONTs (1 0 0): -3.62×10^4 • Cu-MONTs (1 1 1): 4.88×10^4 • Cu-MONTs (2 1 0): 2.89×10^5	At an initial concentration of 50 mg/L, maximum adsorption capacities were: • Dibutyl phthalate (DBP): 128 • Parachlorometaxylenol (PCMX): 184	Li et al. (2021) [53].

Table 4. *Cont.*

Adsorbent	Study Domain	Simulation Environment Operating Conditions	Surface Area (m^2/g)	Simulation Result	Adsorption Capacity (mg/g)	References
Molecular imprinting material (C-MIL-100-MIP)	Design, mechanism and application for improvement of selective catalytic oxidation capacity of phthalates from surface molecular-imprinted catalysis materials	300 K–600 K	144	• The optimized imprinted catalytic materials had good catalytic capacity on phthalates at a lower PS addition level • When PS: PAEs (n:n) = 11:1, the amount of DEP that could be removed was up to 31.2 mg g^{-1}	Diethyl phthalate adsorption on molecular imprinting material (C-MIL-100-MIP) was 19.1	Li 2021 02 [54].

In the view of research related to the simulation study of wastewater treatment using the metal–organic framework (MOF), it was found that different MOF exhibited different binding properties for the same pollutant. In the simulation study of androgens and progestogens removal from water, four other MOFs, i.e., MIL-101(Cr), MIL-100(Fe), MIL-53(Al) and UiO-66(Zr) were studied [48]. The binding energies were calculated for these adsorbents, and it was found that UiO-66(Zr) had the highest adsorption capacity with a binding energy of -7.96 kcal/mol. The surface of the adsorbent played a significant role in the adsorption process. In the simulation study for the adsorption of endocrine-disrupting compounds and the pharmaceuticals/personal care products study conducted by Li et al. (2021) [53], they revealed that the adsorption energies of the DBP/MONTs (hkl) interfaces were dependent upon the surface. The values obtained for the (0 0 -1), (1 0 0), (1 1 1) and (2 1 0) surfaces were reported to be 2.60×10^5, -3.62×10^4, 4.88×10^4 and 2.89×10^5 kcal/mol, respectively.

In a study on the capture of pesticides from wastewater using the Zeolitic imidazolate framework [18], the loading value of prothiofos and ethion obtained for the ZIF-8 unit cell with a size of $2 \times 2 \times 2$ was 14 and 11 molecules, while for ZIF-67, there were 10 and 9 molecules, respectively. So, the adsorption capacities of prothiofos onto ZIF-8 and ZIF-67 were 366.7 and 261.1 mg/g, respectively. ZIF-8 proved to be a better adsorbent for prothiofos contaminants and also for ethions with an adsorption capacity of 279.3 mg/g. Firouzjaei et al. (2020) [50] and Abdelhameed et al. (2021) [51] observed adsorption energies to estimate its capacity for contaminant removal. Firouzjaei et al. (2020) [50] studied the graphene oxide-copper-metal organic framework nanocomposite for dye removal, as shown in Figure 5, and obtained an adsorption energy of -323 and -119 kcal/mol for GO-Cu-MOF and Cu-MOF, respectively. GO-Cu-MOF served as a better adsorbent than Cu-MOF for dye removal from water. Abdelhameed et al. (2021) [51] studied amino-functionalized Al-MIL-53 for the adsorption of a dimethoate pesticide, in which the adsorption energies were calculated for two surfaces of Al-MOF. In their study, it was found that the MOFs (001) surface had greater adsorption energy than the MOFs (100) surfaces. The maximum adsorption energy was obtained using Al-BDC-NH$_2$ at -31.4 and -46.1 kcal/mol for surfaces 001 and 100, respectively. The adsorption energies were increased with BDC-NH$_2$ contents as HBs formed between MOF-amine groups with the dimethoate molecules.
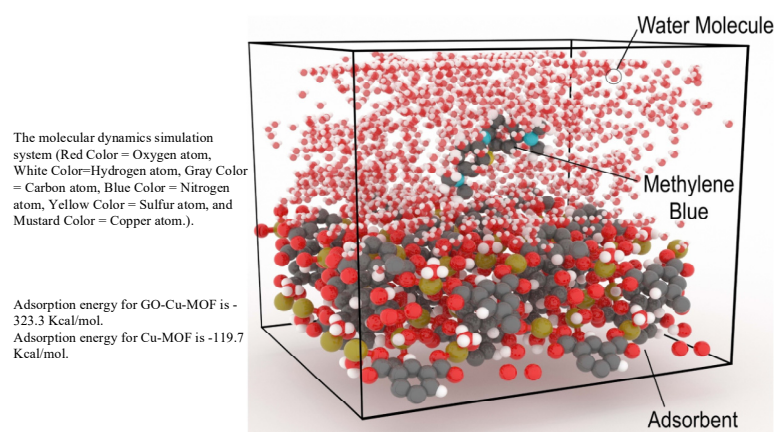

Figure 5. Illustration for adsorption system of methylene blue removal using metal-organic framework on simulation software. Reprinted with permission from Ref. [50] Copyright 2021 Elsevier, Firouzjaei et al., 2022.

2.5. Clay

Among all adsorbents, clay is the most commonly used and inexpensive adsorbent. It is naturally available and widely used in water and wastewater treatment fields [52–54]. The simulation studies using different clay compounds for wastewater treatment are summarized in Table 5.

Table 5. The simulation study using different clay compounds for wastewater treatment.

Adsorbent	Study Domain	Simulation Environment Operating Conditions	Surface Area (m²/g)	Simulation Result	Adsorption Capacity (mg/g)	References
Organo-bentonite	Adsorption isotherms modeling and molecular simulation for adsorption mechanism of methylene blue onto organo-bentonite	60 °C	84.6	Van der Waals forces (VWF) in kcal/mol were: • Bentonite: 12,750.27 • Rarasaponin: 138.586	321	Bergaoui et al. (2018) [55].
Gemini surfactant modified layered montmorillonite	Efficient preparation and molecular dynamic (MD) simulations of Gemini surfactant modified layered montmorillonite to potentially adsorb organic contaminants from wastewater	NA	• Ca-Mt: 48.728 • G-Mt: 8.505	The loading of 16-3-16 increased from 1.0 to 1.5 CEC (Cation Exchange Capacity).	Maximum adsorption capacities on Ca-Mt-1.0 at equilibrium were: • HOBT: 25.93 • BTA: 18.31 • TTA: 16.24	Li et al. (2019) [56].
Natural montmorillonite	Molecular simulation and adsorbent characterization studies for the mechanism of amitriptyline adsorption on natural montmorillonite through batch adsorption	303 K	NA	The calculated occupied areas of AMI molecules and CEC (Cation Exchange Capacity in (meq/g) were: • 60.0 Å: 0.7 • 30.0 Å: 0.15 • 15.0 Å: 0.30 • 10.0 Å: 0.44 • 7.6 Å: 0.58 • 6.2 Å: 0.71 • 5.2 Å: 0.84 • 4.7 Å: 0.94 • 4.3 Å: 1.02	Maximum AMI adsorption at pH 7–8 was 276 mg/g	Chang et al. (2021) [57].
Kaolinite	Molecular insights to understand removal of pharmaceutical residues from wastewater on kaolinite surfaces	NA	NA	Adsorption energy in kJ/mol were: • Paracetamol (PAR): −159.4 • Ibuprofen (IBU): −154.8 • Carbamazepine (CAR): −137.7 • Aspirin (ASP): −46.2 • Diclofenac (DIC): −114.2 • Diazepam (DIA): −96.8	NA	Hounfodji et al. (2021) [58].

Table 5. *Cont.*

Adsorbent	Study Domain	Simulation Environment Operating Conditions	Surface Area (m²/g)	Simulation Result	Adsorption Capacity (mg/g)	References
Magnetic montmorillonite composite γ-Fe$_2$O$_3$@Mt	Experimental and molecular dynamics simulation study for removal of Rhodamine B dye on magnetic montmorillonite composite γ-Fe$_2$O$_3$@Mt	NA	NA	The adsorption energy of a single RhB molecule adsorbed on the maghemite (311) nanosurface was −1259.9 kcal/mol	The maximum adsorption amount of RhB was 209.20	Ouachtak et al., 2020 [59].
Organo-montmorillonite	Experimental study and molecular dynamics to understand adsorption of orange G dye from polluted water using superb organo-montmorillonite	298 K	CTAB@Mt: 52	The adsorption energies in kcal/mol were • OG molecule and CTAB@Mt: −109.8 for the outer surface • OG molecule and CTAB@Mt: −78.6 kcal within interlayer space • Raw Mt: −60.6	Using Langmuir isotherm, the maximum adsorption capacity calculated was 167	Ouachtak et al., 2021 [60].
Montmorillonite	Study of removal of sulfamethoxazole and tetracycline using montmorillonite in single and binary systems	298 K	NA	As the TC concentration increased, the d001-spacing changes were: • 2 mmol/L: 16.4 Å • 4 mmol/L: 21.9 Å.	NA	Wu et al. (2019) [4].
Kaolinite	Molecular dynamics simulation and density functional theory to investigate the interaction between xanthate and kaolinite based on experiments	298 K	NA	The adsorption energies in kJ/mol were: • Kaol (001) surface: 52.33 • Kaol (00i) surface:29.65	NA	Zhang et al. (2021) [21].

The molecular dynamics simulation for clay as an adsorbent uncovered the various factors that affected the adsorption phenomenon. Bergaoui et al. (2018) [55] studied the adsorption mechanism of methylene blue onto organo-bentonite and found that the adsorption of MB occurs on the bentonite as well as on the rarasaponin parts. No hydrogen bonding was observed. Van der Waals forces were repulsive for rarasaponin/MB with a strong electrostatic interaction with and attraction for bentonite/MB with zero electrostatic forces, in which Bentonite was calculated to be 12,750.27 kcal/mol while rarasaponin was 138.586 kcal/mol. Ouachtak et al. (2020) [59] calculated the adsorption energy for the sorption of Rhodamine B dye on the magnetic montmorillonite composite γ-Fe_2O_3@Mt. Their results showed that the adsorption energy of a single RhB molecule adsorbed on the maghemite (311) nanosurface, as shown in Figure 6, was the lowest among the five studied surfaces with a value of -1259.9 kcal·mol^{-1}, indicating that it was most preferred for RhB removal. According to Hounfodji et al. (2020) [58], clay was a cheap and good quality adsorbent with a regeneration ability for pharmaceutical wastewater treatment in comparison to carbon-based compounds, i.e., activated carbon, which had a low regeneration ability with expensive preparation methods. In the research study for molecular insights on the adsorption of some pharmaceutical residues (structures are shown in Figure 6 from wastewater on kaolinite surface), it was found that paracetamol was strongly adsorbed on kaolinite with an adsorption energy of -159.4 kJ/mol.

(Red Color = Oxygen atom, White Color =Hydrogen atom, Gray Color = Carbon atom, Blue Color = Nitrogen atom)
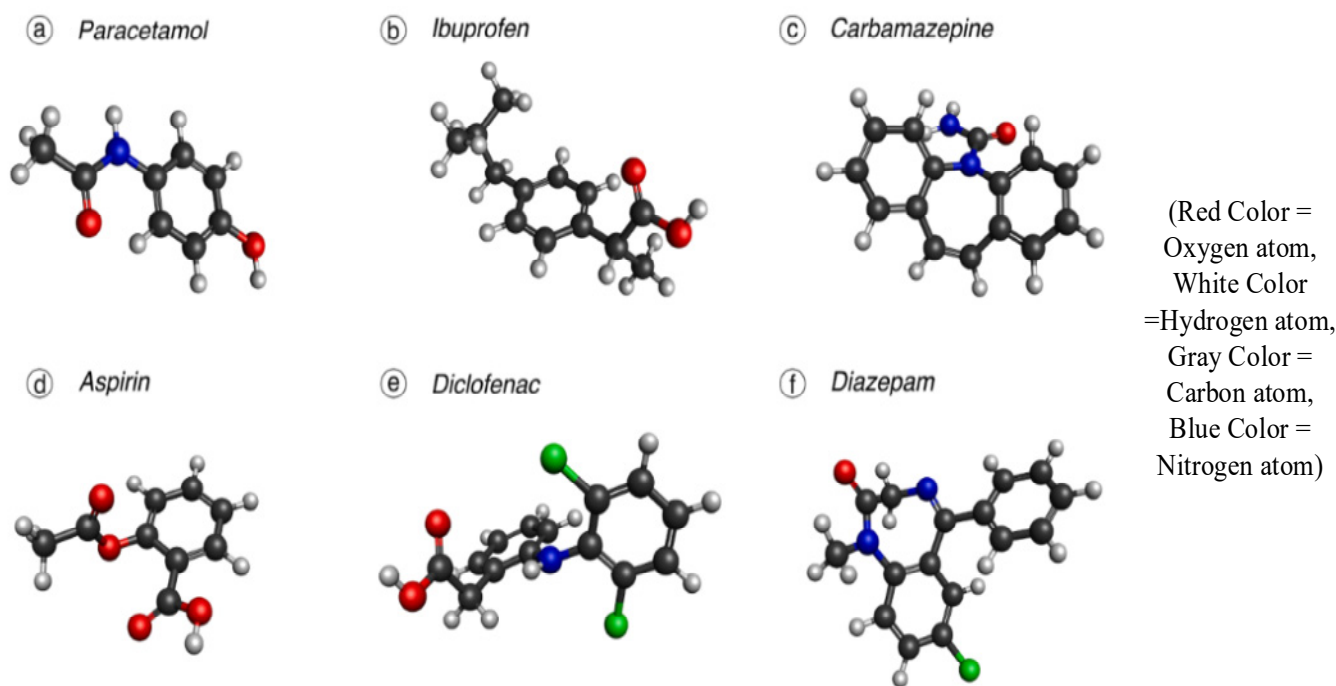
Figure 6. Illustration of different structures of pharmaceutical residues for simulation study using clay. Reprinted with permission from Ref. [58] Copyright 2020 Elsevier, Hounfodji et al., 2020.3. Challenges and Future Directions.

No doubt, many improvements have been observed in the adsorption process with the modification and studying of adsorbents, but the diversity and operating range of studies are still limited. The study of adsorbents is highly attractive for future considerations due to their advantages of being portable and easy to maintain. There are very few simulation studies discussing adsorbent regeneration and reuse. Most of the spent adsorbents can be potentially recovered, regenerated, and further managed through reuse or safe disposal. But it may not be something potentially plausible to be conducted using molecular simulation at the moment due to challenges such as technical barriers in molecular modeling, including adsorbent aging, the plant operational environment, etc. [35]. In addition, this can be attributed to a limitation of the molecular simulation approach to model equilibrated

chemical reactions and differences in the time scale between the simulation window and the actual regeneration process for properly sampling and equilibrating these systems. There are some simulation studies discussing adsorbent recovery using thermodynamic properties. Delgadillo-Velasco (2018) [17] stated in their study that for phosphates removal from water using molecular simulation studies, iron(III) hydroxide allowed the formation of the complex $\equiv FePO_4H_2$, with a Gibbs free energy of -21.38 kcal/mol, and could again become FeOOH, which showed that it was possible to recover the phosphates and reuse them later. The separation of contaminants from the adsorbent would provide adsorbents for reuse.

In addition, there are still limited studies regarding the screening of adsorbents using molecular simulations for different contaminants such as heavy metal elements (i.e., mercury, arsenic, etc.) removal to represent varying water resources. Therefore, more future works are necessary to predict the performance of the adsorption process for contaminant removal from water and to investigate it under a broad range of operating conditions. It will help better understand the adsorption mechanism on various adsorbents using a feasible and low-cost research approach to help select the best material for a specific application. Over and above, molecular simulations can also serve in exploring new adsorbents in the field of water and wastewater treatment.

3. Conclusions

In conclusion, the review of molecular simulation studies helps in understanding the adsorption studies for different adsorbents. It was seen that the adsorption process is remarkably successful at removing different categories of pollutants (such as dyes, pharmaceutical residues, organic pollutants) present in wastewater. Each adsorbent has its pros and cons, and it was seen that the adsorption capacity depends on several factors such as energies (binding and Gibbs free), interactions, molecular arrangement, orientation and operating conditions. Molecular dynamic simulations unveil these factors for a better understanding of the adsorption process. It was found from the review that adsorption studies are mostly conducted under a specific simulation condition. This comprehensive review analysis also revealed that there are still existing gaps in the applicability of simulation studies in the field of water treatment, such as the removal of toxic metal contaminants for various adsorbents from different classes.

Industrial wastewater is detrimental to public health and every country observes EPA (Environmental Protection Agency) guidelines for the correct disposal of wastewater to protect the environment. That is why almost every industry seeks better and more valuable methods of wastewater treatment in order to ensure a safe environment for society. If adsorbents are screened using molecular simulation studies, this can create a pathway for the feasible implementation of a wastewater treatment plant's installation and operation for every industry. The best adsorbent will be used for efficient operation according to the type of wastewater. This review helps with selecting the best adsorbent according to the type of wastewater. The findings of this review also highlight the importance of the interaction of the adsorbent with the contaminant for the adsorption phenomenon and also the vitality of the selection of a specific adsorbent with corresponding toxic matter. This review has also discussed the significance of using a suitable adsorbent for efficient operation in accordance with the type of wastewater.

Institutional Review Board Statement: Not applicable.

Informed Consent Statement: Not applicable.

Data Availability Statement: No data were used for the research described in the article.

Conflicts of Interest: The authors declare no conflict of interest.

References

1. Bayantong, A.R.B.; Shih, Y.J.; Ong, D.C.; Abarca, R.R.M.; Dong, C.D.; de Luna, M.D.G. Adsorptive removal of dye in wastewater by metal ferrite-enabled graphene oxide nanocomposites. *Chemosphere* **2021**, *274*, 129518. [CrossRef] [PubMed]
2. Yagub, M.T.; Sen, T.K.; Afroze, S.; Ang, H.M. Dye and its removal from aqueous solution by adsorption: A review. *Adv. Colloid Interface Sci.* **2014**, *209*, 172–184. [CrossRef] [PubMed]
3. Badeenezhad, A.; Azhdarpoor, A.; Bahrami, S.; Yousefinejad, S. Removal of methylene blue dye from aqueous solutions by natural clinoptilolite and clinoptilolite modified by iron oxide nanoparticles. *Mol. Simul.* **2019**, *45*, 564–571. [CrossRef]
4. Wu, M.; Zhao, S.; Tang, M.; Jing, R.; Shao, Y.; Liu, X.; Dong, Y.; Li, M.; Liao, Q.; Lv, G.; et al. Adsorption of sulfamethoxazole and tetracycline on montmorillonite in single and binary systems. *Colloids Surfaces A Physicochem. Eng. Asp.* **2019**, *575*, 264–270. [CrossRef]
5. Ba Mohammed, B.; Yamni, K.; Tijani, N.; Alrashdi, A.A.; Zouihri, H.; Dehmani, Y.; Chung, I.M.; Kim, S.H.; Lgaz, H. Adsorptive removal of phenol using faujasite-type Y zeolite: Adsorption isotherms, kinetics and grand canonical Monte Carlo simulation studies. *J. Mol. Liq.* **2019**, *296*, 111997. [CrossRef]
6. Hemavathy, R.V.; Saravanan, A.; Kumar, P.S.; Vo, D.V.N.; Karishma, S.; Jeevanantham, S. Adsorptive removal of Pb(II) ions onto surface modified adsorbents derived from Cassia fistula seeds: Optimization and modelling study. *Chemosphere* **2021**, *283*, 131276. [CrossRef]
7. Kuhlman, T.; Farrington, J. What is sustainability? *Sustainability* **2010**, *2*, 3436–3448. [CrossRef]
8. Kumari, P.; Alam, M.; Siddiqi, W.A. Usage of nanoparticles as adsorbents for waste water treatment: An emerging trend. *Sustain. Mater. Technol.* **2019**, *22*, e00128. [CrossRef]
9. Walker, G.M.; Weatherley, L.R. Textile wastewater treatment using granular activated carbon adsorption in fixed beds. *Sep. Sci. Technol.* **2000**, *35*, 1329–1341. [CrossRef]
10. Paliulis, D. Removal of formaldehyde from synthetic wastewater using natural and modified zeolites. *Pol. J. Environ. Stud.* **2016**, *25*, 251–257. [CrossRef]
11. Lin, S.H.; Juang, R.S. Adsorption of phenol and its derivatives from water using synthetic resins and low-cost natural adsorbents: A review. *J. Environ. Manage.* **2009**, *90*, 1336–1349. [CrossRef] [PubMed]
12. McKay, G.; Ramprasad, G.; Pratapa Mowli, P. Equilibrium studies for the adsorption of dyestuffs from aqueous solutions by low-cost materials. *Water Air Soil Pollut.* **1986**, *29*, 273–283. [CrossRef]
13. Pérez Jiménez, V.A.; Hernández-Montoya, V.; Ramírez-Montoya, L.A.; Castillo-Borja, F.; Tovar-Gómez, R.; Montes-Morán, M.A. Adsorption of impurities from nickel-plating baths using commercial sorbents to reduce wastewater discharges. *J. Environ. Manag.* **2021**, *284*, 112024. [CrossRef] [PubMed]
14. Wanyonyi, F.S.; Fidelis, T.T.; Mutua, G.K.; Orata, F.; Pembere, A.M.S. Role of pore chemistry and topology in the heavy metal sorption by zeolites: From molecular simulation to machine learning. *Comput. Mater. Sci.* **2021**, *195*, 110519. [CrossRef]
15. Asif, K.; Lock, S.S.M.; Taqvi, S.A.A.; Jusoh, N.; Yiin, C.L.; Chin, B.L.F. A molecular simulation study on amine-functionalized silica/polysulfone mixed matrix membrane for mixed gas separation. *Chemosphere* **2023**, *311*, 136936. [CrossRef]
16. Zhang, J.; Lu, X.; Shi, C.; Yan, B.; Gong, L.; Chen, J.; Xiang, L.; Xu, H.; Liu, Q.; Zeng, H. Unraveling the molecular interaction mechanism between graphene oxide and aromatic organic compounds with implications on wastewater treatment. *Chem. Eng. J.* **2019**, *358*, 842–849. [CrossRef]
17. Delgadillo-Velasco, L.; Hernández-Montoya, V.; Rangel-Vázquez, N.A.; Cervantes, F.J.; Montes-Morán, M.A.; del Rosario Moreno-Virgen, M. Screening of commercial sorbents for the removal of phosphates from water and modeling by molecular simulation. *J. Mol. Liq.* **2018**, *262*, 443–450. [CrossRef]
18. Abdelhameed, R.M.; Taha, M.; Abdel-Gawad, H.; Mahdy, F.; Hegazi, B. Zeolitic imidazolate frameworks: Experimental and molecular simulation studies for efficient capture of pesticides from wastewater. *J. Environ. Chem. Eng.* **2019**, *7*, 103499. [CrossRef]

19. Chang, S.; Zhang, Q.; Lu, Y.; Wu, S.; Wang, W. High-efficiency and selective adsorption of organic pollutants by magnetic CoFe2O4/graphene oxide adsorbents: Experimental and molecular dynamics simulation study. *Sep. Purif. Technol.* **2020**, *238*, 116400. [CrossRef]

20. Meng, Z.; Wu, M.; Yu, Y.; Meng, F.; Liu, A.; Komarneni, S.; Zhang, Q. Selective removal of methyl orange and Cr anionic contaminants from mixed wastewater by in-situ formation of Zn-Al layered double hydroxides. *Appl. Clay Sci.* **2018**, *161*, 1–5. [CrossRef]

21. Zhang, X.; Zhao, Y.; Zhang, Z.; Wang, S. Investigation of the interaction between xanthate and kaolinite based on experiments, molecular dynamics simulation, and density functional theory. *J. Mol. Liq.* **2021**, *336*, 116298. [CrossRef]

22. Zhang, Q.; Han, Y.; Wu, L. Influence of electrostatic field on the adsorption of phenol on single-walled carbon nanotubes: A study by molecular dynamics simulation. *Chem. Eng. J.* **2019**, *363*, 278–284. [CrossRef]

23. Pelalak, R.; Soltani, R.; Heidari, Z.; Malekshah, R.E.; Aallaei, M.; Marjani, A.; Rezakazemi, M.; Kurniawan, T.A.; Shirazian, S. Molecular dynamics simulation of novel diamino-functionalized hollow mesosilica spheres for adsorption of dyes from synthetic wastewater. *J. Mol. Liq.* **2021**, *322*, 114812. [CrossRef]

24. Khanmohammadi, H.; Bayati, B.; Rahbar Shahrouzi, J.; Babaluo, A.A.; Ghorbani, A. Molecular simulation of the ion exchange behavior of Cu2+, Cd2+ and Pb2+ ions on different zeolites exchanged with sodium. *J. Environ. Chem. Eng.* **2019**, *7*, 103040. [CrossRef]

25. Pelalak, R.; Soltani, R.; Heidari, Z.; Malekshah, R.E.; Aallaei, M.; Marjani, A.; Rezakazemi, M.; Shirazian, S. Synthesis, molecular dynamics simulation and adsorption study of different pollutants on functionalized mesosilica. *Sci. Rep.* **2021**, *11*, 1967. [CrossRef]

26. Liu, X.; Tu, Y.; Liu, S.; Liu, K.; Zhang, L.; Li, G.; Xu, Z. Adsorption of ammonia nitrogen and phenol onto the lignite surface: An experimental and molecular dynamics simulation study. *J. Hazard. Mater.* **2021**, *416*, 125966. [CrossRef]

27. Tuzen, M.; Sarı, A.; Afshar Mogaddam, M.R.; Kaya, S.; Katin, K.P.; Altunay, N. Synthesis of carbon modified with polymer of diethylenetriamine and trimesoyl chloride for the dual removal of Hg (II) and methyl mercury ([CH$_3$Hg]+) from wastewater: Theoretical and experimental analyses. *Mater. Chem. Phys.* **2022**, *277*, 125501. [CrossRef]

28. Hossain, S.; Rahman, M.S.; Dhar, L.; Quraishi, S.B.; Abser, M.N.; Rahman, F.; Rahman, M.T. Increasing the potentiality of graphene oxide by chloroacetic acid for the adsorption of lead with molecular dynamic interpretation. *Curr. Res. Green Sustain. Chem.* **2021**, *4*, 100095. [CrossRef]

29. Dryaz, A.R.; Shaban, M.; AlMohamadi, H.; Al-Ola, K.A.A.; Hamd, A.; Soliman, N.K.; Ahmed, S.A. Design, characterization, and adsorption properties of Padina gymnospora/zeolite nanocomposite for Congo red dye removal from wastewater. *Sci. Rep.* **2021**, *11*, 21058. [CrossRef]

30. Taylor, P.; Siepmann, J.I. Configurational bias Monte Carlo: A new sampling scheme for flexible chains. *Mol. Phys.* **2013**, *75*, 37–41.

31. Metropolis, N.; Rosenbluth, A.W.; Rosenbluth, M.N.; Teller, A.H.; Teller, E. Equation of state calculations by fast computing machines. *J. Chem. Physics* **1953**, *21*, 1087–1092. [CrossRef]

32. Tao, Y.R.; Zhang, G.H.; Xu, H.J. Grand canonical Monte Carlo (GCMC) study on adsorption performance of metal organic frameworks (MOFs) for carbon capture. *Sustain. Mater. Technol.* **2022**, *32*, e00383. [CrossRef]

33. Levy, M. Universal variational functionals of electron densities, first-order density matrices, and natural spin-orbitals and solution of the v-representability problem. *Proc. Natl. Acad. Sci. USA* **1979**, *76*, 6062–6065. [CrossRef]

34. Wu, Z.; Zhou, J.; Li, D.; Ao, Z.; An, T.; Wang, G. Density functional theory study on the enhanced adsorption mechanism of gaseous pollutants on Al-doped Ti2CO2 monolayer. *Sustain. Mater. Technol.* **2021**, *29*, e00294. [CrossRef]

35. Yee, C.Y.; Lim, L.G.; Lock, S.S.M.; Jusoh, N.; Yiin, C.L.; Chin, B.L.F.; Chan, Y.H.; Loy, A.C.M.; Mubashir, M. A systematic review of the molecular simulation of hybrid membranes for performance enhancements and contaminant removals. *Chemosphere* **2022**, *307*, 135844. [CrossRef]

36. Huang, B.; Zhao, R.; Xu, H.; Deng, J.; Li, W.; Wang, J.; Yang, H.; Zhang, L. Adsorption of Methylene Blue on Bituminous Coal: Adsorption Mechanism and Molecular Simulation. *ACS Omega* **2019**, *4*, 14032–14039. [CrossRef]

37. Galdino, A.L.; Oliveira, J.C.A.; Magalhaes, M.L.; Lucena, S.M.P. Prediction of the phenol removal capacity from water by adsorption on activated carbon. *Water Sci. Technol.* **2021**, *84*, 135–143. [CrossRef]

38. Han, Y.; Wang, N.; Guo, X.; Jiao, T.; Ding, H. Influence of ultrasound on the adsorption of single-walled carbon nanotubes to phenol: A study by molecular dynamics simulation and experiment. *Chem. Eng. J.* **2022**, *427*, 131819. [CrossRef]

39. Zhang, L.; Sun, Y. Molecular simulation of adsorption and its implications to protein chromatography: A review. *Biochem. Eng. J.* **2010**, *48*, 408–415. [CrossRef]

40. Li, L.; He, M.; Feng, Y.; Wei, H.; You, X.; Yu, H.; Wang, Q.; Wang, J.X. Adsorption of xanthate from aqueous solution by multilayer graphene oxide: An experimental and molecular dynamics simulation study. *Adv. Compos. Hybrid. Mater.* **2021**, *4*, 725–732. [CrossRef]

41. Theiss, F.L.; Ayoko, G.A.; Frost, R.L. Removal of boron species by layered double hydroxides: A review. *J. Colloid Interface Sci.* **2013**, *402*, 114–121. [CrossRef] [PubMed]

42. Dhar, L.; Hossain, S.; Rahman, M.S.; Quraishi, S.B.; Saha, K.; Rahman, F.; Rahman, M.T. Adsorption Mechanism of Methylene Blue by Graphene Oxide-Shielded Mg-Al-Layered Double Hydroxide from Synthetic Wastewater. *J. Phys. Chem. A* **2021**, *125*, 954–965. [CrossRef] [PubMed]

43. Cao, Y.; Malekshah, R.E.; Heidari, Z.; Pelalak, R.; Marjani, A.; Shirazian, S. Molecular dynamic simulations and quantum chemical calculations of adsorption process using amino-functionalized silica. *J. Mol. Liq.* **2021**, *330*, 115544. [CrossRef]

44. Ma, Y.; Chew, J.W. Investigation of membrane fouling phenomenon using molecular dynamics simulations: A review. *J. Membr. Sci.* **2022**, *661*, 120874. [CrossRef]

45. Jiang, N.; Erdős, M.; Moultos, O.A.; Shang, R.; Vlugt, T.J.H.; Heijman, S.G.J.; Rietveld, L.C. The adsorption mechanisms of organic micropollutants on high-silica zeolites causing S-shaped adsorption isotherms: An experimental and Monte Carlo simulation study. *Chem. Eng. J.* **2020**, *389*, 123968. [CrossRef]

46. Capa-Cobos, L.F.; Jaramillo-Fierro, X.; González, S. Computational study of the adsorption of phosphates as wastewater pollutant molecules on faujasites. *Processes* **2021**, *9*, 1821. [CrossRef]

47. Damjanović, L.; Rakić, V.; Rac, V.; Stošić, D.; Auroux, A. The investigation of phenol removal from aqueous solutions by zeolites as solid adsorbents. *J. Hazard. Mater.* **2010**, *184*, 477–484. [CrossRef]

48. Gao, G.; Xing, Y.; Liu, T.; Wang, J.; Hou, X. UiO-66 (Zr) as sorbent for porous membrane protected micro-solid-phase extraction androgens and progestogens in environmental water samples coupled with LC-MS/MS analysis: The application of experimental and molecular simulation method. *Microchem. J.* **2019**, *146*, 126–133. [CrossRef]

49. Bigdeli, A.; Khorasheh, F.; Tourani, S.; Khoshgard, A.; Bidaroni, H.H. Molecular Simulation Study of the Adsorption and Diffusion Properties of Terephthalic Acid in Various Metal Organic Frameworks. *J. Inorg. Organomet. Polym. Mater.* **2020**, *30*, 1643–1652. [CrossRef]

50. Dadashi Firouzjaei, M.; Akbari Afkhami, F.; Rabbani Esfahani, M.; Turner, C.H.; Nejati, S. Experimental and molecular dynamics study on dye removal from water by a graphene oxide-copper-metal organic framework nanocomposite. *J. Water Process Eng.* **2020**, *34*, 101180. [CrossRef]

51. Abdelhameed, R.M.; Taha, M.; Abdel-Gawad, H.; Hegazi, B. Amino-functionalized Al-MIL-53 for dimethoate pesticide removal from wastewater and their intermolecular interactions. *J. Mol. Liq.* **2021**, *327*, 114852. [CrossRef]

52. Hong, T.Z.X.; Dahanayaka, M.; Liu, B.; Law, A.W.K.; Zhou, K. Zeolitic imidazolate frameworks as capacitive deionization electrodes for water desalination and Cr(VI) adsorption: A molecular simulation study. *Appl. Surf. Sci.* **2021**, *546*, 149080. [CrossRef]

53. Li, Q.; Zhu, S.; Hao, G.; Hu, Y.; Wu, F.; Jiang, W. Fabrication of thermoresponsive metal–organic nanotube sponge and its application on the adsorption of endocrine-disrupting compounds and pharmaceuticals/personal care products: Experiment and molecular simulation study. *Environ. Pollut.* **2021**, *273*, 116466. [CrossRef]

54. Li, X.; Wan, J.; Wang, Y.; Ding, S.; Sun, J. Improvement of selective catalytic oxidation capacity of phthalates from surface molecular-imprinted catalysis materials: Design, mechanism, and application. *Chem. Eng. J.* **2021**, *413*, 127406. [CrossRef]

55. Bergaoui, M.; Nakhli, A.; Benguerba, Y.; Khalfaoui, M.; Erto, A.; Soetaredjo, F.E.; Ismadji, S.; Ernst, B. Novel insights into the adsorption mechanism of methylene blue onto organo-bentonite: Adsorption isotherms modeling and molecular simulation. *J. Mol. Liq.* **2018**, *272*, 697–707. [CrossRef]

56. Li, P.; Khan, M.A.; Xia, M.; Lei, W.; Zhu, S.; Wang, F. Efficient preparation and molecular dynamic (MD) simulations of Gemini surfactant modified layered montmorillonite to potentially remove emerging organic contaminants from wastewater. *Ceram. Int.* **2019**, *45*, 10782–10791. [CrossRef]

57. Chang, P.H.; Liu, P.; Sarkar, B.; Mukhopadhyay, R.; Yang, Q.Y.; Tzou, Y.M.; Zhong, B.; Li, X.; Owens, G. Unravelling the mechanism of amitriptyline removal from water by natural montmorillonite through batch adsorption, molecular simulation and adsorbent characterization studies. *J. Colloid Interface Sci.* **2021**, *598*, 379–387. [CrossRef]

58. Hounfodji, J.W.; Kanhounnon, W.G.; Kpotin, G.; Atohoun, G.S.; Lainé, J.; Foucaud, Y.; Badawi, M. Molecular insights on the adsorption of some pharmaceutical residues from wastewater on kaolinite surfaces. *Chem. Eng. J.* **2021**, *407*, 127176. [CrossRef]

59. Ouachtak, H.; El, R.; El, A.; Haounati, R.; Amaterz, E.; Ait, A.; Akbal, F.; Labd, M. Experimental and molecular dynamics simulation study on the adsorption of Rhodamine B dye on magnetic montmorillonite composite γ-Fe$_2$O$_3$@Mt. *J. Mol. Liq.* **2020**, *309*, 113142. [CrossRef]

60. Ouachtak, H.; El Guerdaoui, A.; Haounati, R.; Akhouairi, S.; El Haouti, R.; Hafid, N.; Ait Addi, A.; Šljukić, B.; Santos, D.M.F.; Taha, M.L. Highly efficient and fast batch adsorption of orange G dye from polluted water using superb organo-montmorillonite: Experimental study and molecular dynamics investigation. *J. Mol. Liq.* **2021**, *335*, 116560. [CrossRef]